1.5-THz eight-step FZP and ordinary lenses/antennas become comparable in focusing intensity/gain action. This result is not due to a superior radiation performance of the FZP lens but mostly to the big absorption loss in the bulky ordinary lenses at terahertz waves. Finally, by use of a new design approach to the terahertz grooved-dielectric FZP lens the unwanted focusing shift from the design frequency is removed and better focusing performance is obtained.

The FZP lenses are much smaller in thickness, volume, and weight than the ordinary lenses and this leads to a creation of lighter lens antennas. Besides, the diffractive plane-step FZP lenses are easy for production and have better fabrication-error tolerance. The application of terahertz FZP lenses and antennas includes pico-range communication systems, radio telescopes, and imaging and security systems among many others.

ACKNOWLEDGMENTS

The authors acknowledge the support on this work of the Chilean Scientific Conicyt Agency under the Research Projects Fondecyt 1095012/2009 and 1095018/2009 and Anillos ACT-53/2009 all executed at Departamento de Electrónica, Universidad Técnica Federico Santa María, Valparaíso.

REFERENCES

1. J. Ojeda-Castaneda and C. Gómes-Reino (Eds.), Selected papers on zone plates, SPIE Opt. Edging Press, Washington, 1996.
2. F. Sobel, F.L. Wentworth, and J.C. Wiltse, Quasi-optical, surface waveguide and other components for the 100- to 300-Gc region, I.R.E. Trans Microwave Theory Tech MTT-9 (1961), 512–518.
3. J.C. Wiltse, The Fresnel zone-plate lens, Proceedings of SPIE Symposium, Vol. 544, 1985, 41–47.
4. D.N. Black and J.C. Wiltse, Millimeter-wave characteristics of phase-correcting Fresnel zone plates, IEEE Trans Microwave Theory Tech 35 (1987), 1122–1129.
5. J.M. Houten and M.H.A.J. Herben, Analysis of phase-correcting Fresnel-zone plate antenna with dielectric/transparent zones, J Electromagn Wave Appl 8 (1994), 847–858.
6. H.D. Hristov, Analysis and design of transmissive fresnel zone antennas for DBS reception, CEC CIPA 35 10CT926503 Report, Division of Telecommunications, Eindhoven University of Technology, Feb. 1994.
7. H.D. Hristov and M.H.A.J. Herben, Millimeter-wave Fresnel zone plate lens and antenna, IEEE Trans Microwave Theory Tech 43 (1995), 2770–2785.
8. P.F. Goldsmith, Quasioptical systems, Wiley, New York, NY, 1998.
9. H.D. Hristov, Fresnel zones in wireless links, zone plate lenses and antennas, Artech House, Boston-London, 2000.
10. O.V. Minin and I.V. Minin, Diffractive optics of millimeter waves, IoP Publisher, Boston-London, 2004.
11. D.R. Reid and G.S. Smith, A full electromagnetic analysis of grooved-dielectric fresnel zone plate antennas for microwave and millimeter-wave applications, IEEE Trans Antennas Propag 55 (2007), 2138–2146.
12. J. Wiltse, Diffractional optics for terahertz waves, Proceedings of SPIE Symposium, Vol. 5411, Orlando, F1, 2004, 127–135
13. J.C. Wiltse, Zone plate designs for terahertz frequencies, Proceedings of SPIE Symposium, Vol. 5790, Bellingham, WA, pp. 167–179, 2005.
14. S. Wang et al., Characterization of T-ray binary lenses, Opt Lett 27 (2002), 1183–1185.
15. E.D. Walsby et al., Multilevel silicon diffractive optics for terahertz waves, J Vac Sci Technol B 20 (2002), 2780–2783.
16. CST microwave studio, CST Computer simulation technology AG, Version 10, 2010.

SMALL-SIZE WWAN TABLET COMPUTER ANTENNA WITH DISTRIBUTED AND LUMPED PARALLEL RESONANT CIRCUITS

Kin-Lu Wong and Ying-Chieh Liu
Department of Electrical Engineering, National Sun Yat-Sen University, Kaohsiung 804, Taiwan; Corresponding author: wongkl@ema.ee.nsysu.edu.tw

Received 9 August 2011

ABSTRACT: *The technique of embedding a distributed parallel resonant circuit (PRC) and a lumped PRC, respectively, to enhance the bandwidths of the lower and upper bands of a small-size tablet computer antenna to cover the WWAN operation in the 824–960 and 1710–2170 MHz bands is presented. With the proposed technique, the antenna occupies a small volume of 40 × 10 × 3.8 mm^3 only and can mainly be disposed on a thin FR4 substrate of 40 × 10 mm^2. The antenna comprises a feeding portion, a long shorted strip, and an antenna ground. The shorted strip is short-circuited to the antenna ground, which is then connected to the display ground in the tablet computer. A lumped PRC and a distributed PRC are added at the front and open ends of the feeding portion, respectively. The two PRCs, respectively, generate a parallel resonance at the high-frequency tails of the first two resonant modes at about 900 and 1800 MHz contributed by the shorted strip to result in additional resonances occurred near the two resonant modes, thereby resulting in additional resonant modes excited in the desired antenna's lower and upper bands. This behavior greatly increases the operating bandwidths of the antenna's lower and upper bands, without additional resonant elements needed. Hence, small size for the proposed WWAN antenna is obtained. Details of the proposed antenna and the bandwidth enhancement techniques applied therein are presented.* © 2012 Wiley Periodicals, Inc. Microwave Opt Technol Lett 54:1348–1353, 2012; View this article online at wileyonlinelibrary.com. DOI 10.1002/mop.26811

Key words: *mobile antennas; tablet computer antennas; WWAN antennas; parallel resonant circuit; bandwidth enhancement*

1. INTRODUCTION

To achieve two wide operating bands at about 900 and 1900 MHz to cover the GSM850/900 and GSM1800/1900/UMTS operation, respectively, in the tablet computer with a large display ground, the embedded antenna generally requires to have a large size (typically at least 50 mm in length) along the display ground edge [1–15]. This is mainly because the chassis (ground plane) mode of the tablet computer generally cannot be excited to assist in achieving a wide lower band for the embedded antenna in the tablet computer, which is different from that in the mobile handset [16–18]. Hence, the use of at least two or multiple radiating elements (strip monopole or shorted strip monopole elements in Refs. 1–9, monopole slot elements in Refs. 10 and 11, and loop elements or combo strip monopole/loop elements in Refs. 12–15) is generally required to generate multiple resonant modes for the reported internal tablet computer or laptop computer antennas. The at least two radiating elements make the occupied volume not easy to be reduced to achieve a compact antenna size.

In this article, we demonstrate a small-size internal WWAN antenna using a single radiating shorted strip monopole element for the tablet computer application. The antenna volume is 40 × 10 × 3.8 mm^3 only, and its planar size of 40 × 10 mm^2 in the plane parallel to the display ground of the tablet computer is about the smallest among the reported WWAN antennas for the tablet computer or laptop computer applications. To excite the

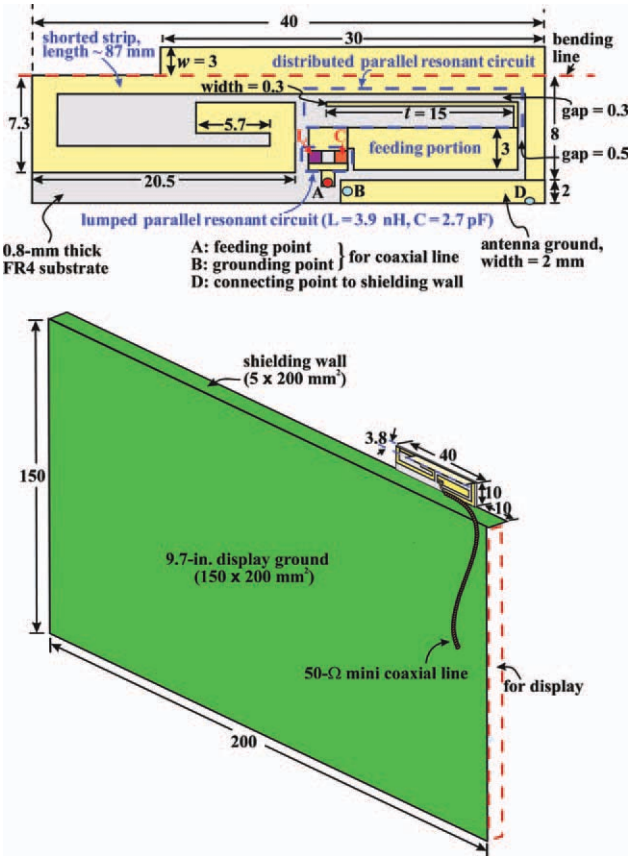

Figure 1 Geometry of the proposed WWAN tablet computer antenna with distributed and lumped PRCs. [Color figure can be viewed in the online issue, which is available at wileyonlinelibrary.com]

shorted strip, a feeding portion encircled therein and loaded with a distributed parallel resonant circuit (PRC) and a lumped PRC is applied. As the feeding portion is encircled by the shorted strip and is not a resonant element to contribute resonant modes, the feeding portion can have a small size to help decrease the occupied size of the proposed antenna. The two added PRCs can, respectively, generate a parallel resonance [19] at the high-frequency tails of the first two resonant modes at about 900 and 1800 MHz contributed by the shorted strip to result in additional resonances occurred near the two resonant modes. The additional resonances lead to additional resonant modes generated in the desired antenna's lower and upper bands. Hence, the operating bandwidths of the antenna's lower and upper bands are greatly enhanced, without the use of additional resonant elements. Small size for the proposed WWAN antenna is also obtained. Detailed operating principle of the bandwidth enhancement using the proposed distributed and lumped PRCs is described in the article. The proposed antenna is fabricated and tested. Results of the proposed antenna are presented and discussed.

2. PROPOSED ANTENNA

Figure 1 shows the geometry of the proposed WWAN tablet computer antenna. The antenna is mainly printed on a 0.8-mm thick FR4 substrate of size 40 × 10 mm^2. The antenna comprises a feeding portion, a long shorted strip, and an antenna ground. The shorted strip is short circuited to the antenna ground, which is connected to the display ground in the tablet computer as shown in the figure. The display ground has a size of 150 × 200 mm^2, about the same size as that of a 9.7-in. tablet computer on the market [20]. The antenna is mounted vertically at the shielding metal wall (size 5 × 200 mm^2) along the top edge of the display ground. The shielding wall is used to accommodate the internal antennas and may also decrease possible coupling between the antennas and the display. The antenna is also placed at a distance of 10 mm to one corner of the shielding wall to allow more possible internal antennas to be mounted along the shielding wall. In practical applications, there are usually a variety of internal antennas required to be embedded in the tablet computer.

The antenna ground of the proposed antenna is electrically connected to the shielding wall at point D. The shorted strip has a length of 90 mm and is short circuited to the antenna ground. The shorted strip can contribute its first two resonant modes at about 900 and 1800 MHz, and there is a widened section of width (w) 3 mm and length 30 mm connected to the shorted strip to improve the bandwidths of the two excited resonant modes. The widened section is oriented to be parallel to the shielding wall and is cut from a 0.2-mm thick copper plate in the experiment. The shorted strip is also extended substantially as a rectangular spiral strip to minimize the antenna size. Also note that with the open end of the shorted strip (where there is generally strong near-field electric field because of null surface currents) encircled within the shorted strip, it can be expected that possible coupling between the antenna and other embedded antennas (if any) nearby can be minimized.

The feeding portion is also encircled by the shorted strip. The central part of the feeding portion is a simple rectangular strip of size 3 × 13 mm^2. At its front end, a lumped PRC is added, whereas at its open end, a distributed PRC is disposed. The lumped PRC consists of a 3.9-nH chip inductor and a 2.7-pF chip capacitor, both connected in parallel. This lumped PRC can generate a first parallel resonance at about 1200 MHz, which is at the high-frequency tail of the resonant mode at about 900 MHz generated by the shorted strip. The first parallel resonance will cause an additional resonance (zero reactance) at about 1000 MHz, which leads to an additional resonant mode occurred to combine the one at about 900 MHz to form a wide lower band for the antenna to cover the GSM850/900 operation (824–960 MHz).

The distributed PRC is formed by a long narrow (width 0.3 mm) strip closely coupled to the shorted strip with a coupling gap of width 0.3 mm. The long narrow strip provides a distributed inductance [21], whereas the coupling between the section (length t in the figure) of the narrow strip and the shorted strip provides a distributed capacitance [22]. This distributed PRC leads to a second parallel resonance generated at about 2650 MHz. This parallel resonance can result in an additional resonance occurred at about 2150 MHz, which is at the high-frequency tail of the resonant mode at about 1800 MHz. An additional resonant mode nearby the one at about 1800 MHz can hence be generated, and both are formed into a wide upper band for the antenna to cover the GSM1800/1900/UMTS operation (1710–2170 MHz).

To feed the antenna, a 50-Ω mini coaxial line is used, whose central conductor and outer grounding sheath is connected to point A (front end of the lumped PRC) and point B at the antenna ground, respectively. The antenna is also fabricated and tested. The photograph of the fabricated antenna is shown in Figure 2, and obtained results of the proposed antenna are presented and discussed in Section 3.

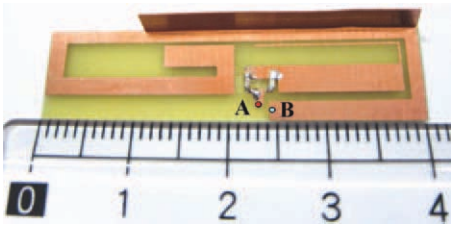

Figure 2 Photograph of the fabricated antenna. [Color figure can be viewed in the online issue, which is available at wileyonlinelibrary.com]

3. RESULTS OF PROPOSED ANTENNA

Figure 3 shows the measured and simulated return loss for the proposed antenna. Two wide operating bands to cover the desired lower and upper bands for the penta-band WWAN operation (the shaded regions in the figure) are obtained. The impedance matching for frequencies over the desired lower and upper bands is better than 3:1 VSWR or 6-dB return loss, which is the widely used design specification of the internal WWAN antenna for mobile devices [23–25]. Good agreement between the measured data and the simulated results obtained using full-wave electromagnetic field simulator, high-frequency structure simulator (HFSS; Ref. 26), is observed.

Note that for both the lower and the upper bands, two resonant modes are excited. The second modes in both the lower and the upper bands are excited mainly owing to the two parallel resonances generated by the distributed and lumped PRCs in the feeding portion. This behavior can be seen more clearly from the simulated input impedance for the proposed antenna shown in Figure 4. The first and second parallel resonances are generated at about 1200 and 2650 MHz, respectively. The first parallel resonance results in a new resonance at about 1000 MHz and leads to the second resonant mode excited in the antenna's lower band. The second parallel resonance also results in a new resonance, which is at about 2150 MHz and leads to the second resonant mode excited in the antenna's upper band. The dual-resonance behavior in both the lower and the upper bands leads to enhanced bandwidths to cover the desired 824–960 and 1710–2170 MHz bands.

The respective effects of the lumped and distributed PRCs are also analyzed. Figure 5 shows the simulated return loss and input impedance for the proposed antenna and the case without the distributed PRC. As shown in Figure 5(a) for the simulated return loss, when the distributed PRC is not present, the second resonant mode in the antenna's upper band disappears and the

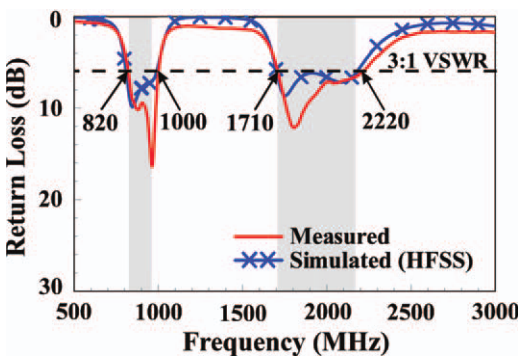

Figure 3 Measured and simulated return loss for the proposed antenna. [Color figure can be viewed in the online issue, which is available at wileyonlinelibrary.com]

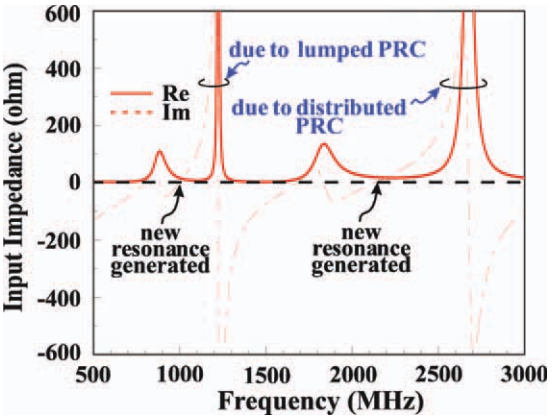

Figure 4 Simulated input impedance for the proposed antenna. [Color figure can be viewed in the online issue, which is available at wileyonlinelibrary.com]

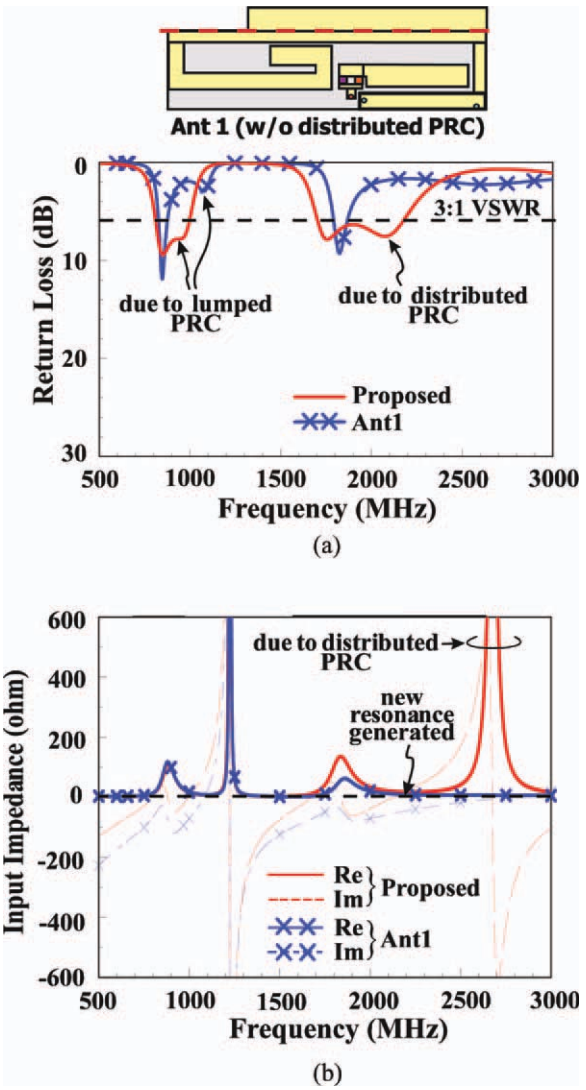

Figure 5 Simulated (a) return loss and (b) input impedance for the proposed antenna and the case without the distributed PRC (Ant1). [Color figure can be viewed in the online issue, which is available at wileyonlinelibrary.com]

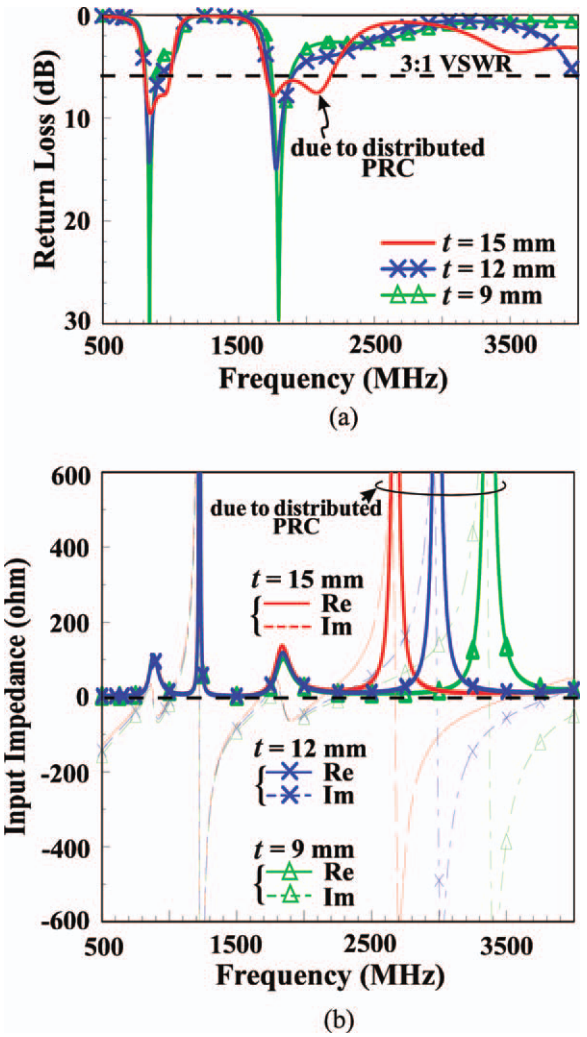

Figure 6 Simulated (a) return loss and (b) input impedance as a function of the length t in the distributed PRC. [Color figure can be viewed in the online issue, which is available at wileyonlinelibrary.com]

first resonant mode also becomes narrow banded. This behavior can be confirmed from the simulated input impedance shown in Figure 5(b), in which it is seen the second parallel resonance at about 2650 MHz disappears when the distributed PRC is not present. On the other hand, the second resonant mode in the lower band is still present, although it shows poor impedance matching. It can also be seen that there are some variations in the first parallel resonance occurred at about 1200 MHz [see Fig. 5(b)], when the distributed PRC is not present. The results indicate that the distributed PRC will also have some effects on the first parallel resonance generated by the lumped PRC.

Figure 6 shows the simulated return loss and input impedance as a function of the length t in the distributed PRC. Results for the length t varied from 15 to 9 mm are presented. Results show that the second parallel resonance can be controlled by adjusting the length t, because it can lead to some variations in both the distributed inductance and the capacitance in the distributed PRC. With a properly selected length t, good excitation of the second resonant mode in the upper band can be obtained. It can also improve the impedance matching of the first resonant mode in the upper band.

Effects of the lumped PRC are analyzed. Figure 7 shows the simulated return loss and input impedance for the proposed antenna and the case without the lumped PRC. From the simulated input impedance shown in Figure 6(b), the first parallel resonance disappears when the lumped PRC is not present. Accordingly, the bandwidth of the antenna's lower band is greatly decreased. Although the second parallel resonance is generated by the distributed PRC, the input impedance of the first resonant mode in the upper band is also affected by the absence of the lumped PRC. In this case, dual-resonance excitation cannot be obtained in the upper band as well [see Fig. 7(a)]. The results indicate that the lumped PRC will also cause some effects on the impedance matching for frequencies over the upper band.

Figure 8 shows the simulated return loss as a function of the width w of the widened section in the shorted strip. Results for the width w varied from 1 to 3 mm are presented. Improvements on the impedance matching of the antenna' lower and upper bands are seen. Hence, the presence of the widened section in the shorted strip is helpful in widening the antenna's operating bandwidth.

Measured radiation characteristics of the proposed antenna are presented in Figures 9 and 10. The antenna was measured in

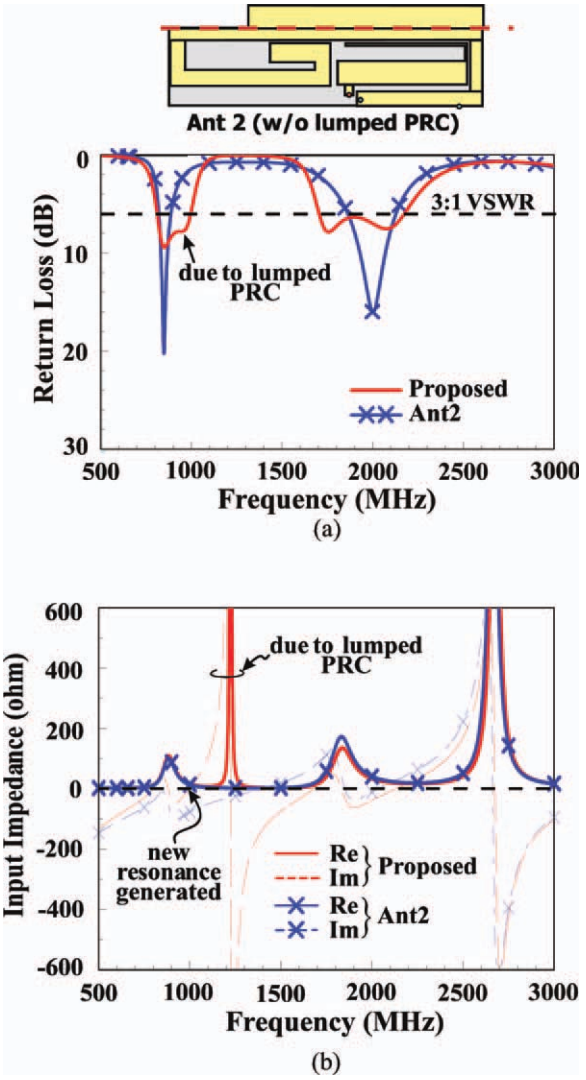

Figure 7 Simulated (a) return loss and (b) input impedance for the proposed antenna and the case without the lumped PRC (Ant2). [Color figure can be viewed in the online issue, which is available at wileyonlinelibrary.com]

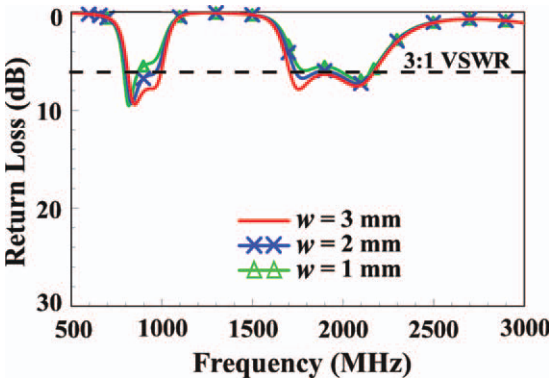

Figure 8 Simulated return loss as a function of the width w of the widened section in the shorted strip. [Color figure can be viewed in the online issue, which is available at wileyonlinelibrary.com]

a far-field anechoic chamber, and the measured antenna efficiency includes the mismatching loss. As shown in Figure 9, the measured antenna efficiency is about 52–69% and 50–64% over the GSM850/900 and GSM1800/1900/UMTS bands, respectively. The obtained antenna efficiency is acceptable for practical applications [27]. The measured three-dimensional (3D) radiation patterns of the proposed antenna are plotted in Figure 10. The full 3D patterns and half 3D patterns with the cross-sectional cut at the x–z plane at five representative frequencies in the antenna's lower and upper bands are shown. The radiation patterns at lower frequencies of 859 and 925 MHz are no longer close to dipole-like patterns as seen for the internal handset antennas [28–33]. This is mainly because the display ground of the tablet computer is relatively much larger than the system ground plane of the mobile handset or smartphone. For all the radiation patterns obtained at lower and higher frequencies, large asymmetry in the radiation patterns is also seen. The radiation in the half-plane in the $-y$ direction is seen to be stronger than that in the $+y$ direction. This behavior is related to the excited surface currents excited on the display ground, which leads to the asymmetric radiation patterns observed.

4. CONCLUSIONS

A WWAN tablet computer antenna using distributed and lumped PRCs to achieve small size ($40 \times 10 \times 3.8$ mm^3) and wideband

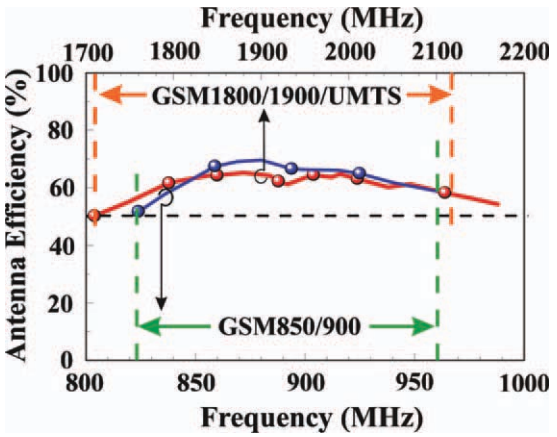

Figure 9 Measured antenna efficiency (mismatching loss included) of the proposed antenna. [Color figure can be viewed in the online issue, which is available at wileyonlinelibrary.com]

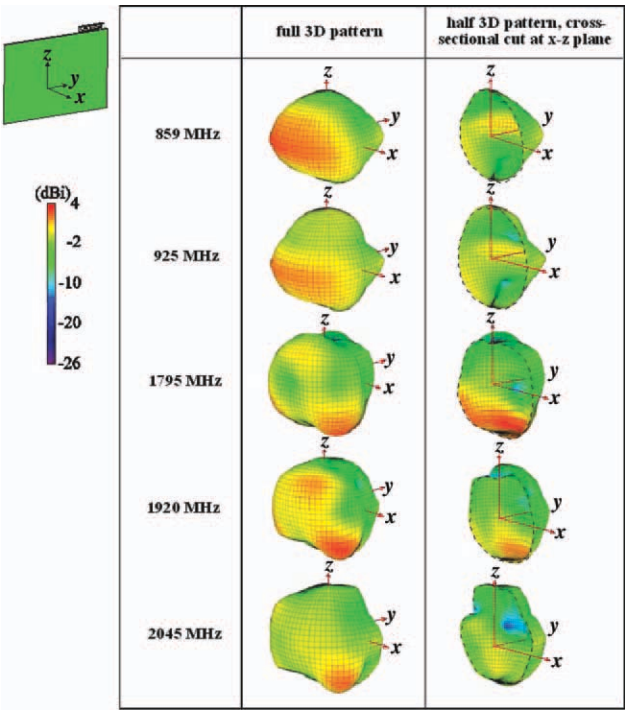

Figure 10 Measured radiation patterns of the proposed antenna. [Color figure can be viewed in the online issue, which is available at wileyonlinelibrary.com]

operation (824–960/1710–2170 MHz) has been proposed and experimentally studied. The distributed and lumped PRCs can generate two parallel resonances to result in two new resonant modes excited in the desired antenna's lower and upper band, thereby greatly enhancing the operating bandwidths of the antenna. Detailed effects of the bandwidth enhancement using the distributed and lumped PRCs have been studied. Good radiation characteristics over the WWAN operating bands have also been obtained. With the obtained results, the proposed antenna is promising for practical tablet computer applications.

REFERENCES

1. X. Wang, W. Chen, and Z. Feng, Multiband antenna with parasitic branches for laptop applications, Electron Lett 43 (2007), 1012–1013.
2. C.H. Chang and K.L. Wong, Internal coupled-fed shorted monopole antenna for GSM850/900/1800/1900/UMTS operation in the laptop computer, IEEE Trans Antennas Propagat 56 (2008), 3600–3604.
3. C. Zhang, S. Yang, S. El-Ghazaly, A.E. Fathy, and V.K. Nair, A low-profile branched monopole laptop reconfigurable multiband antenna for wireless applications, IEEE Antennas Wireless Propagat Lett 8 (2009), 216–219.
4. K.L. Wong and S.J. Liao, Uniplanar coupled-fed printed PIFA for WWAN operation in the laptop computer, Microwave Opt Technol Lett 51 (2009), 549–554.
5. C.W. Chiu, Y.J. Chi, and S.M. Deng, An internal multiband antenna for WLAN and WWAN applications, Microwave Opt Technol Lett 51 (2009), 1803–1807.
6. C.T. Lee and K.L. Wong, Study of a uniplanar printed internal WWAN laptop computer antenna including user's hand effects, Microwave Opt Technol Lett 51 (2009), 2341–2346.
7. C.L. Hu, D.L. Huang, H.L. Kuo, C.F. Yang, C.L. Liao, and S.T. Lin, Compact multibranch inverted-F antenna to be embedded in a laptop computer for LTE/WWAN/IMT-E applications, IEEE Antennas Wireless Propagat Lett 9 (2010), 838–841.

8. T.W. Kang, K.L. Wong, L.C. Chou, and M.R. Hsu, Coupled-fed shorted monopole with a radiating feed structure for eight-band LTE/WWAN operation in the laptop computer, IEEE Trans Antennas Propagat 59 (2011), 674–679.
9. T.W. Kang and K.L. Wong, Simple two-strip monopole with a parasitic shorted strip for internal eight-band LTE/WWAN laptop computer antenna, Microwave Opt Technol Lett 53 (2011), 706–712.
10. K.L. Wong and L.C. Lee, Multiband printed monopole slot antenna for WWAN operation in the laptop computer, IEEE Trans Antennas Propagat 57 (2009), 324–330.
11. K.L. Wong and F.H. Chu, Internal planar WWAN laptop computer antenna using monopole slot elements, Microwave Opt Technol Lett 51 (2009), 1274–1279.
12. Y.W. Chi, T.W Chiu, and F.R. Hsiao, Printed penta-band laptop computer antenna for WWAN operation, In: 2009 Asia-Pacific microwave conference proceedings, Singapore, pp.1987–1989.
13. K.L. Wong, W.J. Chen, L.C. Chou, and M.R. Hsu, Bandwidth enhancement of the small-size internal laptop computer antenna using a parasitic open slot for the penta-band WWAN operation, IEEE Trans Antennas Propagat 58 (2010), 3431–3435.
14. T.W. Kang and K.L. Wong, Internal printed loop/monopole combo antenna for LTE/GSM/UMTS operation in the laptop computer, Microwave Opt Technol Lett 52 (2010), 1673–1678.
15. K.L. Wong and P.J. Ma, Coupled-fed loop antenna with branch radiators for internal LTE/WWAN laptop computer antenna, Microwave Opt Technol Lett 52 (2010), 2662–2667.
16. P. Vainikainen, J. Ollikainen, O. Kivekas, and I. Kelander, Resonator-based analysis of the combination of mobile handset and chassis, IEEE Trans Antennas Propagat 50 (2002), 1433–1444.
17. T.Y. Wu and K.L. Wong, On the impedance bandwidth of a planar inverted-F antenna for mobile handsets, Microwave Opt Technol Lett 32 (2002), 249–251.
18. Y.W. Chi and K.L. Wong, Compact multiband folded loop chip antenna for small-size mobile phone, IEEE Trans Antennas Propagat 56 (2008), 3797–3803.
19. Y.W. Chi and K.L. Wong, Very-small-size folded loop antenna with a band-stop matching circuit for WWAN operation in the mobile phone, Microwave Opt Technol Lett 51 (2009), 808–814.
20. K.L. Wong and W.J. Lin, Body SAR study of the planar WWAN monopole slot antenna for tablet device application, Microwave Opt Technol Lett 53 (2011), 1721–1727.
21. C.H. Chang and K.L. Wong, Small-size printed monopole with a printed distributed inductor for penta-band WWAN mobile phone application, Microwave Opt Technol Lett 51 (2009), 2903–2908.
22. K.L. Wong and C.H. Huang, Bandwidth-enhanced internal PIFA with a coupling feed for quad-band operation in the mobile phone, Microwave Opt Technol Lett 50 (2008), 683–687.
23. H.W. Hsieh, Y.C. Lee, K.K. Tiong, and J.S. Sun, Design of a multiband antenna for mobile handset operations, IEEE Antennas Wireless Propagat Lett 8 (2009), 200–203.
24. X. Zhang and A. Zhao, Bandwidth enhancement of multiband handset antennas by opening a slot on mobile handset, Microwave Opt Technol Lett 51 (2009), 1702–1706.
25. C.L. Liu, Y.F. Lin, C.M. Liang, S.C. Pan, and H.M. Chen, Miniature internal penta-band monopole antenna for mobile phones, IEEE Trans Antennas Propagat 58 (2010), 1008–1011.
26. ANSYS HFSS Available at: http://www.ansys.com/products/hf/hfss/.
27. A. Andújar, J. Anguera, and C. Puente, Ground plane boosters as a compact antenna technology for wireless handheld devices, IEEE Trans Antennas Propagat 59 (2011), 1668–1677.
28. W. Yu, S. Yang, C.L. Tang, and D. Tu, Accurate simulation of the radiation performance of a mobile slide phone in a hand-held position, IEEE Antennas Propagat Mag 52 (2010), 168–177.
29. K.L. Wong, W.Y. Chen, and T.W. Kang, On-board printed coupled-fed loop antenna in close proximity to the surrounding ground plane for penta-band WWAN mobile phone, IEEE Trans Antennas Propagat 59 (2011), 751–757.
30. F.H. Chu and K.L. Wong, Simple planar printed strip monopole with a closely-coupled parasitic shorted strip for eight-band LTE/GSM/UMTS mobile phone, IEEE Trans Antennas Propagat 58 (2010), 3426–3431.
31. C.T. Lee and K.L. Wong, Planar monopole with a coupling feed and an inductive shorting strip for LTE/GSM/UMTS operation in the mobile phone, IEEE Trans Antennas Propagat 58 (2010), 2479–2483.
32. Y.W. Chi and K.L. Wong, Quarter-wavelength printed loop antenna with an internal printed matching circuit for GSM/DCS/PCS/UMTS operation in the mobile phone, IEEE Trans Antennas Propagat 57 (2009), 2541–2547.
33. C.H. Chang and K.L. Wong, Printed λ/8-PIFA for penta-band WWAN operation in the mobile phone, IEEE Trans Antennas Propagat 57 (2009), 1373–1381.

A NOVEL BROAD AND MULTIBAND FREQUENCY SELECTIVE SURFACE

Arup Ray, Manisha Kahar, Sushanta Sarkar, Sushanta Biswas, Debashree Sarkar, and Partha P. Sarkar
Department of Engineering and Technological Studies, University of Kalyani, Kalyani, West Bengal, India; Corresponding author: parthabe91@yahoo.co.in

Received 12 August 2011

ABSTRACT: *Simulated theoretical results and experimental verifications are presented for a Frequency selective surface with slotted, perfectly conducting square patch elements. The frequency selective surface (FSS) structure acts like a band-reject filter having three broad stop bands in parts of C, X, and Ku band. Due to symmetrical nature of the design, the FSS is insensitive to variations of RF incidence angle for 90° rotations of the FSS. Simulated theoretical investigations are done by Ansoft Designer® software. Experimental investigation is performed using standard microwave test bench.* © 2012 Wiley Periodicals, Inc. Microwave Opt Technol Lett 54:1353–1355, 2012; View this article online at wileyonlinelibrary.com. DOI 10.1002/mop.26843

Key words: *frequency selective surface; band-reject filter; multifrequency operation; polarization independent*

1. INTRODUCTION

The use of frequency selective surfaces has been successfully proven as a potential means to increase the communication capabilities for satellites [1]. In Voyager, Galileo, and Cassini space missions, the dual-reflector antennas with a frequency selective surface (FSS) subreflector made it possible to share the main reflector among different frequency bands [2–5]. The growing demands on potential multifunctional antennas for radio communications require complex FSS with multiband requirements. Complex multiband FSSs are designed by combining one or more of the following techniques: layered or stacked FSS, perturbation of a single-layered FSS [6], or the use of multiresonant elements such as the concentric rings [7]. The FSS used in Cassini is an example of a complex structure, where two single-layer FSS with multiresonant elements are stacked to obtain the needed performance [8].

In this article, however, we have achieved a multiresonating FSS simply by introducing a slot in each of the square path element of the FSS structure. This technique of obtaining multiple resonant results in a lighter structure, reduced size, less costly, and a simplified design of the FSS, compared to the above-mentioned techniques.

We have analyzed the proposed Frequency Selective Surface structure theoretically by Ansoft Designer® software, which